

Transformation of synthetic mackinawite to hexagonal pyrrhotite: A kinetic study

ALISTAIR R. LENNIE, KATHARINE E. R. ENGLAND, DAVID J. VAUGHAN

Department of Earth Sciences, University of Manchester, Oxford Road, Manchester M13 9PL, U.K.

ABSTRACT

The kinetics of the transformation of synthetically prepared mackinawite to hexagonal pyrrhotite have been studied to clarify the relationship between these two phases. Kinetic analysis using the Johnson-Mehl equation is based on measurements of the fraction of hexagonal pyrrhotite obtained by heating mackinawite samples in the temperature range of 530–545 K. This gives isothermal rate constants from which an activation energy of 493 kJ/mol and a frequency factor of $3.7 \times 10^{45} \text{ min}^{-1}$ have been established. The mechanism proposed for this transformation is that of a solid-state diffusion process.

Kinetic data derived from this experiment may be used to show that persistence of mackinawite in nature can be explained by kinetic factors alone. Reactions at low temperatures, in which mackinawite is oxidized or further sulfidized, are therefore more important than the kinetically inhibited transformation to hexagonal pyrrhotite.

The irreversible mackinawite to hexagonal pyrrhotite relation is compared with the reversible tetragonal FeSe to NiAs-type FeSe phase transformation. This contrast in stability behavior is examined in terms of the thermal stability of the respective tetragonal phases relative to the upper magnetic ordering temperatures of their corresponding hexagonal phases.

INTRODUCTION

In the Fe-S system, phase relations are complex and remain to be fully clarified. This complexity derives in part from the variety of oxidation states and coordination geometries adopted by S. These, in turn, influence the electronic and structural behavior of Fe. To add to this complexity, at low temperatures Fe-S phases form that, despite being metastable, persist long enough to be significant in geological environments.

Examples of iron sulfide metastability are found in the mineral marcasite and the synthetic phase, cubic FeS. These phases transform, spontaneously and isochemically, to pyrite and mackinawite, respectively (Fleet, 1970, 1975; Lennie and Vaughan, 1992; de Médicis, 1970a, 1970b; Takeno et al., 1970; Murowchick and Barnes, 1986). In this study, the relationship between the phases mackinawite (Fe_{1+x}S) and hexagonal pyrrhotite (Fe_{1-x}S) is examined.

The mineral mackinawite (space group $P4/nmm$), first described by Evans et al. (1962, 1964), was shown by Berner (1962, 1964) to be identical to synthetic tetragonal iron monosulfide, t-FeS. Mackinawite has a layer structure similar to that of tetragonal lead monoxide (litharge), with Fe and S occupying the sites occupied by O and Pb, respectively, in litharge. Structural studies using X-ray diffraction (Kouvo et al., 1963; Taylor and Finger, 1970) and neutron (Bertaut et al., 1965) and electron (Uda, 1968) diffraction support this interpretation. Taylor and Finger (1970) suggested that the crystal they studied is S deficient rather than Fe excessive. Iron selenide and iron telluride,

which share the anti-t-PbO structure found in mackinawite, are reported as being metal-excessive chalcogenides (Tsuji et al., 1976).

The term "pyrrhotite" encompasses a wide variety of mineral and synthetic Fe-S phases based on the nickel arsenide structure. In this structure, metal atoms occupy all the octahedral holes in an (approximately) hexagonal close-packed array of anions, while the anions are surrounded by six metal atoms in the form of a trigonal prism. In the case of pyrrhotite, the nickel arsenide-type lattice is modified by structural distortions and Fe vacancies, with consequent changes in magnetic behavior and structure because of vacancy ordering.

At low temperatures, stoichiometric FeS assumes the stable troilite structure, a phase found in iron meteorites and lunar rocks. On Earth, it is found in some serpentinized ultramafic rocks. On the basis of the NiAs-type subcell ($A = 3.45$, $C = 5.8 \text{ \AA}$), the troilite superstructure axial lengths are given as $a = \sqrt{3}A$, $c = 2C$ (Hagg and Sucksdorff, 1933); the space group is $P\bar{6}2c$ (Evans, 1970). Clustering of Fe atoms into prism-like groups appears to stabilize troilite through Fe-Fe bonding. At approximately 420 K (the α transition), the troilite structure breaks down.

The high-temperature phase has been assigned to a NiAs-type structure (Hagg and Sucksdorff, 1933), but more recent work has shown a transitional superstructure intermediate between troilite and the NiAs-type structure (Putnis, 1974; King and Prewitt, 1982; Kruse, 1992), which has been assigned to an orthorhombic MnP-type structure. Kruse (1992) indicated that upon heating of troilite the α transition to the MnP-type superstructure

begins at 373 K and is complete at 413 K; on cooling, the rate of formation of troilite from the MnP structure depends on both the ambient temperature and the thermal history of the sample. King and Prewitt (1982) reported an MnP-NiAs-type transition temperature of 490 ± 20 K.

An electron spin-flip transition occurs in stoichiometric FeS at $T_s = 445$ K. Below this temperature, the antiferromagnetically coupled spins of Fe atoms are aligned parallel to the *c* axis of the NiAs subcell; above this temperature, spins flip to an alignment perpendicular to the *c* axis. The antiferromagnetic order in FeS breaks down into paramagnetism at $T_N = 600$ K (Horwood et al., 1976).

Chemical bonding in t-FeS was discussed by Bertaut et al. (1965), Ward (1970), Kjekshus et al. (1972), Goodenough (1978), and Vaughan and Craig (1978), and electronic band structures of mackinawite were calculated by Welz and Rosenberg (1987); Tsuji et al. (1976) proposed band structures for the equivalent Fe_{1+x}Se structure. Neutron diffraction and Fe Mössbauer measurements on mackinawite show no evidence of magnetic ordering down to 1.7 K, indicating electron delocalization in the structure, and are in agreement with bonding models of mackinawite, which suggest considerable Fe-Fe interaction within mackinawite layers; mackinawite has very short Fe-Fe distances (2.60 Å) within the layers.

Preparation of mackinawite by synthesis from the elements has, in contrast to pyrrhotite synthesis, proved unsuccessful, although Takeno et al. (1982) report exsolution of mackinawite from Cu- or Cu + Co-containing iron sulfide melts annealed at 373, 433, and 458 K for periods of up to 10 months. Mackinawite forms from solution within the range of pH 3–4 to pH 11 by reaction of ferrous ions, or iron metal, with hydrogen sulfide or bisulfide ions. Below pH 3, mackinawite dissolves rapidly, whereas above pH 11, colloidal sodium iron sulfide (NaFeS_2) is formed from solution (Taylor and Shoemith, 1978).

Thermodynamic data on stoichiometric FeS from 298.15 to 1000 K were provided by Grønvold and Stølen (1992), who linked heat capacity measurements with standard enthalpy of formation data for troilite (Cemić and Kleppa, 1988). Thermodynamic measurements on mackinawite are limited to solubility product data, for which the value for $\text{p}K_{\text{sp}}^{\text{NBS}}$ at 298 K for mackinawite is 3.6 ± 0.2 ; $K_{\text{sp}}^{\text{NBS}} = [\text{Fe}^{2+}][\text{HS}^-]_{\gamma}\text{Fe}^{2+}\gamma\text{HS}^- [\text{H}_{\text{NBS}}^+]^{-1}$ (Davison, 1991), where H_{NBS}^+ is derived from pH measured on the NBS scale (Covington et al., 1985). A free energy of formation for mackinawite at 298 K, ΔG_f° (298.15 K) = -87.3 kJ/mol, is estimated from the equation

$$\Delta G_f^\circ(\text{FeS}) = \Delta G_f^\circ(\text{Fe}^{2+}) + \Delta G_f^\circ(\text{HS}^-) - \Delta G_f^\circ(\text{H}^+) + RT \ln K \quad (1)$$

using $\Delta G_f^\circ(\text{Fe}^{2+})_{\text{aq}} = -78.870$ kJ/mol, $\Delta G_f^\circ(\text{HS}^-)_{\text{aq}} = 12.100$ kJ/mol, and $[\Delta G_f^\circ(\text{H}^+)_{\text{aq}} = 0]$ (Robie et al., 1978). This free energy may be compared with ΔG_f° (298.15 K) = -96.7 kJ/mol calculated for troilite from $\text{p}K_{\text{sp}}^{\text{NBS}}$ (298 K) = 5.25 ± 0.2 (Davison, 1991). This indicates that mackinawite is metastable relative to troilite.

Reports of the thermal stability of mackinawite give a conflicting range of values. With natural specimens, the thermal stability has been reported to depend on the effect of substitution of Ni or Co for Fe (Takeno and Clark, 1967; Takeno, 1965a, 1965b; Clark, 1966). These authors proposed a temperature of approximately 413 K as the upper limit of stability of mackinawite, identified by changes in the optical properties of mackinawite as observed by optical microscopy. Zôka et al. (1972) suggested, however, that these observed “breakdown” temperatures of natural mackinawite, in the range 393–426 K, are not isochemical but involve the addition of S from surrounding minerals. In contrast, Kouvo et al. (1963) assigned a small DTA endothermic peak at 518 K for a natural crystal of mackinawite to the transformation to hexagonal pyrrhotite; Sarkar (1971) found that the optical properties of mackinawite change to those of pyrrhotite when mackinawite is heated under vacuum between 493 and 498 K.

The theory that mackinawite is a precursor to pyrite and marcasite nucleation in hydrothermal solutions at temperatures <573 K (Schoonen and Barnes, 1991a, 1991b, 1991c) implies that mackinawite persists for enough time below this temperature to provide a site for pyrite or marcasite formation or both. This study describes an experiment designed to obtain further data on the thermal stability of mackinawite and to investigate the rate and mechanism of transformation of synthetic mackinawite to hexagonal pyrrhotite.

EXPERIMENTAL PROCEDURE

To prepare synthetic mackinawite, 30 mL of a solution of Na_2S (20 g of $\text{Na}_2\text{S} \cdot 9\text{H}_2\text{O}$ in 200 mL deionized water) were added slowly to 500 mL of a 0.5 molar acetic acid + acetate buffer (pH = 4.6), into which approximately 4–5 g of finely divided iron wire had been previously immersed. Partial dissolution of the iron wire in the acetate buffer for 30 min generated H_2 , providing a reducing environment. The Na_2S solution, added slowly, exceeded the capacity of the acetate buffer, increasing the pH to a value of approximately 6.5. This solution, containing the iron wire, was allowed to stand for 24 h. The H_2 generated during dissolution floated the iron to the top of the solution, while mackinawite forming on the iron surface spalled off and dropped to the bottom of the flask, allowing reasonably good separation of mackinawite from the iron.

After reaction, the remaining iron wool was removed and the supernatant solution poured off. The mackinawite was washed onto a $0.45 \mu\text{m}$ filter, then rinsed several times with deaerated deionized water. While still wet, the mackinawite was placed in U-shaped aluminum foil boats approximately 2 cm long, and after crimping both ends of the foil, these boats were inserted into borosilicate tubes. These tubes had been previously sealed at one end using an $\text{O}_2\text{-CH}_4$ flame and partially prefilled with enough acetone to completely cover the inserted aluminium boat. Excess acetone was then removed by pipette.

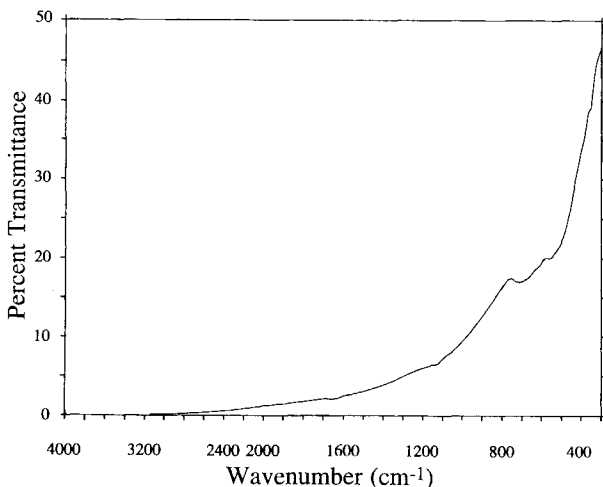


Fig. 1. Infrared transmittance spectrum of mackinawite in KBr. Note the change in wavenumber scale at 2000 cm^{-1} .

Several tubes of mackinawite prepared in this way were dried together under a vacuum of 10^{-2} mbar. Acetone and water were condensed in a liquid N_2 -cooled trap. When dry, each tube was sealed, under vacuum, using an $\text{O}_2\text{-CH}_4$ flame. Sample transfers were made using a glove bag filled with oxygen-free N_2 .

Characterization by X-ray powder diffraction analysis was performed using a Philips X-ray diffractometer, with $\text{CuK}\alpha$ X-rays generated at 40 kV and 20 mA. Samples were mixed with amyl acetate, spread on glass slides, then dried in air. The diffraction pattern of mackinawite shows broad peaks, with the peak width at half peak height $\sim 0.5^\circ 2\theta$; peak positions are consistent with reported diffraction patterns of mackinawite (Kouvo et al., 1963; Berner, 1964). Recorded Mössbauer spectra are consistent with previous reported results (Vaughan and Ridout, 1971; Bertaut et al., 1965).

A sample of mackinawite was prepared for infrared analysis by mixing with spectral grade KBr in the ratio 1:300. This mixture was pressed in an infrared die at 9.5 tons. The spectrum was taken on a Perkin-Elmer 1710 FTIR over the spectral range 4000–300 cm^{-1} , with 50 scans at a resolution of 4 cm^{-1} . The spectrum recorded is shown in Figure 1.

When heated under vacuum, synthetic mackinawite transformed to hexagonal pyrrhotite only, which is consistent with previously reported experimental observations; this transformation was not reversible.

QUANTITATIVE MEASUREMENTS OF TRANSFORMATION

To establish the fraction of mackinawite transformed to hexagonal pyrrhotite with time requires quantitative measurement of both phases. Because the infrared spectra of both mackinawite and pyrrhotite show broad-band

absorption with no sharply defined absorption peaks, quantitative measurement of mackinawite and pyrrhotite fractions after partial transformation using infrared absorption was not possible. Instead, peak area measurements of X-ray diffraction patterns were used.

The intensity of an X-ray reflection is affected by absorption in the specimen as follows (Zussman, 1977):

$$I \approx Kx / \{\rho[x\mu + (1-x)\mu']\} \quad (2)$$

where x = weight fraction of component to be determined, I = intensity of reflection, ρ = density of mixtures, μ = mass absorption coefficient of component to be determined, and μ' = mass absorption coefficient of matrix. Because mackinawite transforms isochemically to hexagonal pyrrhotite in this experiment and $\rho(\text{hexagonal pyrrhotite}) \approx \rho(\text{mackinawite})$, μ is assumed to be equal to μ' , which allows a straight-line relationship between I and x to be obtained.

The kinetics of transformation of synthetic mackinawite to hexagonal pyrrhotite were established by heating samples of mackinawite contained in evacuated borosilicate tubes in a small aluminium block furnace. Measurements of the progress of the transformation were made at three temperatures, 530, 537, and 545 K. Thermocouples were calibrated against the melting points of Pb and Sn. After measured periods of time, the tubes were removed from the furnace and quenched in water to arrest the reaction. It was assumed that the aluminium foil contained in the mackinawite sample tubes did not affect the transformation because no obvious tarnish was observed on the aluminium after the heating experiments.

Standard mixtures of mackinawite and pyrrhotite were prepared by mixing weighed portions of pyrrhotite and unreacted synthetic mackinawite, the pyrrhotite having been previously prepared by heating mackinawite under vacuum at 553 K for 6 h. These conditions ensured complete transformation of mackinawite to pyrrhotite. The molecular weights of mackinawite and the hexagonal pyrrhotite formed from mackinawite were assumed to be identical.

Standard mixtures and samples were all prepared for analysis by diluting one part by weight of iron sulfide with three parts by weight of silicone high-vacuum grease, then mixing the iron sulfide and silicone thoroughly. This procedure was designed to limit oxidation of the iron sulfide. After preparation, samples were stored in a vacuum desiccator. For quantitative analysis, X-ray diffraction measurements were made from the iron sulfide-silicone grease mixture smeared onto glass slides. The sample area was kept the same for all samples by outlining the sample area with tape, then removing the tape after applying the mixture to the slide. Scans were made on the Philips X-ray diffractometer, using $\text{CuK}\alpha$ radiation (40 kV, 20 mA) between 16° and $50^\circ 2\theta$, and measurements of the mackinawite 001 ($17.6^\circ 2\theta$) and the hexagonal pyrrhotite 102 ($43.3^\circ 2\theta$) diffraction peak areas in both standards and samples were made.

An XRD trace of pyrrhotite formed after partial trans-

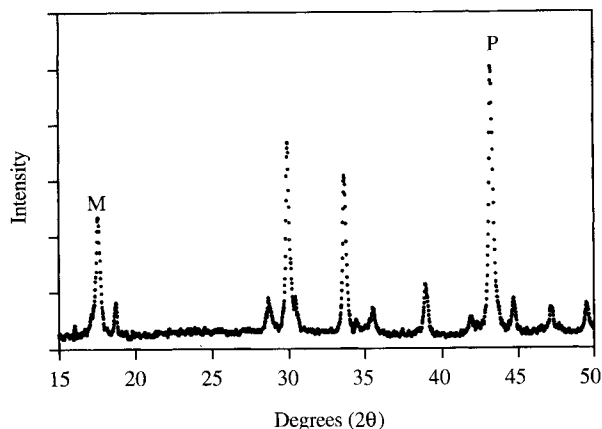


Fig. 2. X-ray diffraction trace of mackinawite after heating under vacuum, showing partial transformation to hexagonal pyrrhotite. Areas under the mackinawite 001 peak ($17.6^\circ 2\theta$, $\text{CuK}\alpha$), labeled M, and the hexagonal pyrrhotite 102 peak ($43.3^\circ 2\theta$), labeled P, were used for quantitative analysis.

formation of mackinawite is shown in Figure 2. Using the calibration formula (Yund and Hall, 1969)

$$\text{at\% Fe} = 45.212 + 72.86(d_{102} - 2.0400) + 311.5(d_{102} - 2.0400)^2 \quad (3)$$

the position of the 102 hexagonal pyrrhotite XRD diffraction peak, $43.3^\circ 2\theta$, gives the composition of the present pyrrhotite as 49.6 ± 0.06 at% Fe.

Standards prepared by mixing end-member mackinawite and pyrrhotite samples have theoretical peak area ratios (γ) given by

$$\gamma = \frac{M_\beta}{P_\beta} \left(\frac{M_\alpha}{1 - M_\alpha} \right) \quad (4)$$

where M_β and P_β are the peak areas of mackinawite and pyrrhotite end-members, respectively, and M_α is the (prepared) fraction of mackinawite in the standard. By rearranging Equation 4 as

$$M_{\alpha(\text{meas})} = \gamma_{\text{meas}}(P_\beta/M_\beta)/[1 + \gamma_{\text{meas}}(P_\beta/M_\beta)] \quad (5)$$

the fraction of mackinawite [$M_{\alpha(\text{meas})}$] in samples and standards is derived from measured peak area ratios (γ_{meas}).

A plot of measured against prepared mackinawite fraction in the standards is shown in Figure 3. A standard (fractional) error of estimate, $\sigma = 0.032$, is calculated from the linear regression for this plot. The pyrrhotite fraction, α , [$1 - M_{\alpha(\text{meas})}$] in the samples is plotted against $\ln t$ in Figure 4.

KINETIC ANALYSIS

A kinetic analysis of these data uses the integrated rate equation

$$\alpha = 1 - \exp[-(kt)^m] \quad (6)$$

known as the Johnson-Mehl or Avrami-Erofe'ev equation (Burke, 1965). In this equation, α is the fraction of

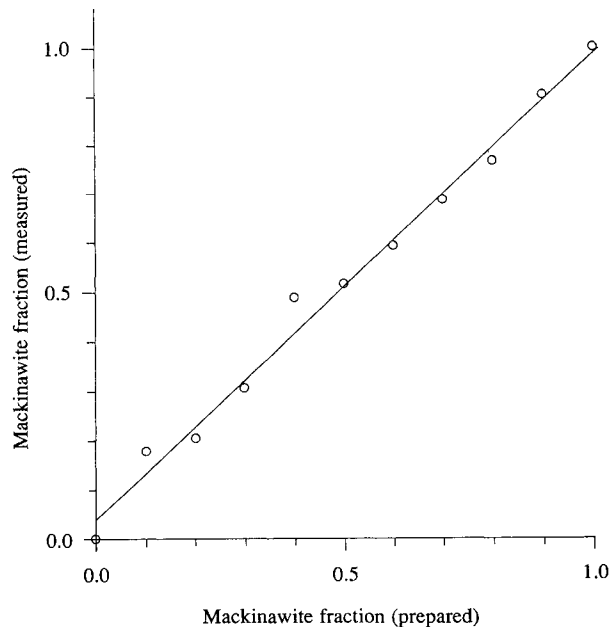


Fig. 3. Calibration graph for standard mixtures of synthetic mackinawite plus hexagonal pyrrhotite. The experimental data are fitted by linear regression, with a slope of 0.947 ± 0.018 , an intercept of 0.040 ± 0.032 , and a correlation coefficient of 0.994.

sample reacted at time t , k is the rate constant of the process, and m is a constant related to the reaction mechanism. If time is plotted on a logarithmic scale, rate curves conforming to Equation 6 show a curve with a shape determined only by m , whereas k fixes the position on the time axis (Redfern, 1987). Figure 4 shows values of α , the fraction of hexagonal pyrrhotite formed from mackinawite, plotted against $\ln t$; the curves are of similar shape, indicating similar kinetic behavior.

Reaction curves having the same shape for a range of experimental temperatures are termed isokinetic and, if the Johnson-Mehl equation is obeyed, have the same value of m . To evaluate m and k , Equation 6 is converted to

$$\ln[-\ln(1 - \alpha)] = m \ln k + m \ln t \quad (7)$$

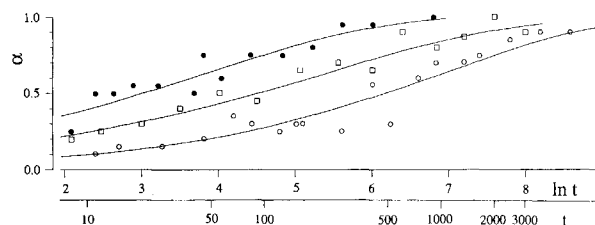


Fig. 4. Fraction of hexagonal pyrrhotite (α) formed by transformation of mackinawite, plotted against logarithm of time (in minutes). Measurements at 545 K are represented by solid circles, at 537 K by open squares, and at 530 K by open circles. The solid curves are derived from the Johnson-Mehl equation, using values of m and k calculated from the experimental data of the present study.

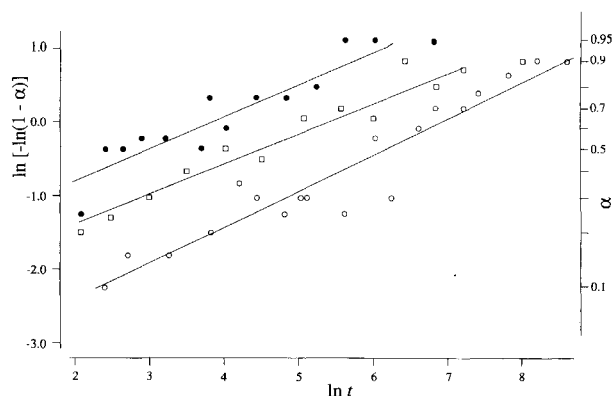


Fig. 5. Plot of $\ln[-\ln(1 - \alpha)]$ against logarithm of time (in minutes), where α is the fraction of hexagonal pyrrhotite formed by transformation of mackinawite. Measurements at 545 K are represented by solid circles, at 537 K by open squares, and at 530 K by open circles. Linear regression fits to these three data sets were used to obtain values for m and k in the Johnson-Mehl equation.

by taking logarithms; the value of m is obtained from the slope of the graph, and $\ln k$ is derived from the y -intercept value. The data from the experiment are plotted in Figure 5, with $\ln t$ as abscissa and $\ln[-\ln(1 - \alpha)]$ as ordinate. Values for m and $\ln k$ obtained from least-squares linear regression analysis of these plots are given in Table 1. These plots show no pronounced curvature, which suggests conformation to the Johnson-Mehl equation throughout the transformation process. Errors (2σ) in the slope (m) and intercept ($m \ln k$) for each temperature were calculated using the 95% confidence limits for the regression coefficient and intercept, respectively (Spiegel, 1991). The error (2σ) in $\ln k$ is calculated by subtracting in quadrature the fractional error in the slope from the fractional intercept error.

Because the values for m are similar at the three temperatures measured, the transformation over this temperature range can be modeled by one kinetic process. By using the logarithmic form of the Arrhenius equation,

$$\ln k = \ln A - E_a/RT \quad (8)$$

values of $\ln k$ obtained from the integrated rate equation are plotted against $1000/T$ (K) (Fig. 6). A linear regression gives an activation energy, E_a , of 493 kJ/mol, derived from the gradient ($-E_a/R$), and a frequency factor, A , of 3.7×10^{45} ($\ln A = 104.9$). An estimate of error in E_a and $\ln A$ is obtained by taking the slopes and intercepts of lines through $Y_A(\text{est})$ at one end temperature and the

TABLE 1. Data from kinetic analysis of $\ln[-\ln(1 - \alpha)]$ plots

T (K)	$1000/T$ (K)	$\ln k(2\sigma)$	$m(2\sigma)$ (slope)	r
545	1.8349	-3.82(31)	0.441(8)	0.9317
537	1.8622	-5.39(20)	0.406(4)	0.9713
530	1.8868	-6.90(28)	0.491(24)	0.9539

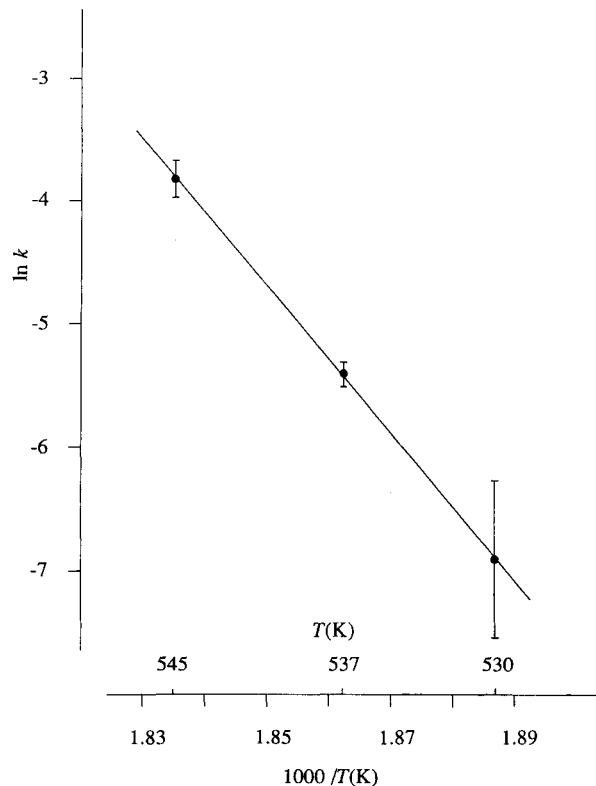


Fig. 6. Arrhenius plot for calculation of the transformation activation energy. Values of k , derived from the Johnson-Mehl equation, are plotted as $\ln k$ against $1000/T$ (K).

points $Y_b(\text{est}) \pm \sigma$ at the other end temperature, where $Y_A(\text{est})$ and $Y_b(\text{est})$ are derived from the linear regression of the plot, and σ is the 68% confidence level in $\ln k$ values. This gives $\ln A$ as 104.9 ± 22.6 (A is bracketed, therefore, by 5.57×10^{35} and 2.41×10^{55}) and E_a as 492 ± 102 kJ/mol.

DISCUSSION

The present experiment gives a temperature range over which synthetic mackinawite rapidly transforms isochemically to hexagonal pyrrhotite that is consistent with, although slightly higher than, the transformation temperatures reported by Kouvo et al. (1963) and Sarkar (1971). A role for mackinawite as the precursor to pyrite in hydrothermal systems up to 573 K (Schoonen and Barnes, 1991a, 1991b, 1991c) requires such a stability range; reports of stability limits for mackinawite in the region of 413 K, as discussed in the introduction, involve oxidation and are therefore not relevant.

Mackinawite was found to transform spontaneously to greigite during exposure to X-rays at elevated temperatures (Lennie, 1994). It is impossible, therefore, to observe directly the expansion of the mackinawite unit cell by X-ray diffraction above about 453 K. However, because the rapid transformation to hexagonal pyrrhotite

does not proceed until about 523 K, it may be assumed that mackinawite persists above 453 K.

Transformation to hexagonal pyrrhotite requires changing the S sublattice from cubic to hexagonal closest packing, and the Fe coordination from fourfold to sixfold. Comparison of m values from the Johnson-Mehl model obtained for this experiment with those tabulated by Hancock and Sharp (1972) indicates that the mechanism for this reconstructive phase transformation is one of diffusion.

The activation energy (493 kJ/mol) obtained in this experiment may be compared with that found for the marcasite to pyrite transformation (253 kJ/mol) (Lennie and Vaughan, 1992). It may be assumed that not all Fe-S bonds are broken in the nucleation of pyrite from marcasite (see Fleet, 1970). Nucleation could occur by breaking of the four planar Fe-S bonds that provide the edge-sharing links between the FeS_6 octahedra in marcasite (Fagot et al., 1981). In comparison, a diffusion process for formation of pyrrhotite from mackinawite may imply that all four Fe-S bonds in mackinawite are broken.

Thus, an estimate of activation energy for the mackinawite to hexagonal pyrrhotite transformation can be made from the marcasite to pyrite activation energy as follows:

$$E_a \approx (0.50/0.33 \times 253 \text{ kJ/mol}) \quad (9)$$

where 0.50 and 0.33 are the atomic fractions of Fe in mackinawite and marcasite, respectively, and 253 kJ/mol is the activation energy established for the marcasite to pyrite transformation. The estimated E_a is 383 kJ/mol, which can be compared with the measured activation energy of 493 kJ/mol for the mackinawite to hexagonal pyrrhotite transformation.

Although this discussion is speculative, both in assuming that the activation energies have a direct relation with bond enthalpies of the two iron sulfide transformations, and that these can be directly compared with each other, the experimental activation energies obtained for these two transformations are of the right order relative to each other. Possible activation energy contributions arising from Fe-Fe bonding in mackinawite or from the differences in S coordination between mackinawite and marcasite are not included in this calculation.

The magnitude of the activation energy describes the temperature dependence of the reaction rate; the value obtained for E_a in the present study is high in comparison with the activation energies of most solid-state processes (Putnis, 1992). The kinetic data obtained in the present study show that, below the temperature range of this experiment, the rate of formation of hexagonal pyrrhotite from mackinawite by solid-state diffusion is extremely slow. The persistence of mackinawite in nature (e.g., meteorites) may therefore be explained by kinetic factors alone; no field of thermodynamic stability for mackinawite need be implied. Although the rate of transformation of mackinawite to hexagonal pyrrhotite may be altered by factors such as high surface area or surface hydrogenation, reactions at lower temperatures, in which mackinawite is oxidized or further sulfidized, are far more im-

portant than the kinetically inhibited transformation to hexagonal pyrrhotite.

The stabilities of mackinawite and hexagonal pyrrhotite may now be compared with the related iron selenide phases. Tetragonal $\text{Fe}_{1.04}\text{Se}$, in contrast to mackinawite, undergoes a reversible transformation to a NiAs-structure FeSe phase at 730.8 K (Grønvold, 1968). Grønvold (1968) proposed that the difference between the heat capacity of $t\text{-Fe}_{1.04}\text{Se}$ and the nontransitional heat capacity of Fe_7Se_8 (which is similar to that of the high-temperature FeSe phase) arises from vibrationally induced electronic transitions in $t\text{-Fe}_{1.04}\text{Se}$ during heating. This effect is modeled by an equation (Schottky, 1922) describing the heat capacity of electronic transitions resulting from removal of (Fe) degeneracy induced by a ligand field.

By analogy with $t\text{-Fe}_{1.04}\text{Se}$, electronic transitions induced by heating may therefore contribute to the heat capacity of mackinawite. Evidence in support of this prediction is provided by the strong infrared absorption observed for mackinawite, as shown in Figure 1. Intense absorption above about 1200 cm^{-1} is consistent with a small band gap between destabilized e energy levels in the Fe d orbitals of mackinawite (Welz and Rosenberg, 1987). Any further development of a heat capacity model for mackinawite would, however, require reliable thermodynamic measurements on this phase at elevated temperatures.

There are no cooperative magnetic phase transitions in $\text{Fe}_{1.04}\text{Se}$ (Tsuji et al., 1976) below the 730.8 K transition temperature, in contrast to Fe_7Se_8 NiAs-type structures where magnetic transitions are observed at 542 and 638 K. A cooperative magnetic transition in $\text{Fe}_{1.04}\text{Se}$, obscured by the tetragonal-hexagonal structural transition (Grønvold, 1968), would occur at a temperature similar to the transition because of the breakdown of long-range order of Fe vacancies (638 K) observed for Fe_7Se_8 . Thus, the tetragonal $\text{Fe}_{1.04}\text{Se}$ to hexagonal FeSe phase transition lies at a temperature well above the magnetic and structural transitions observed for Fe_7Se_8 . On cooling the disordered solid solution of hexagonal FeSe from high temperatures, a gain in order is achieved by formation of the tetragonal $\text{Fe}_{1.04}\text{Se}$ phase at 730.8 K.

In contrast, the first magnetic ordering transition of hexagonal pyrrhotite lies well above the temperature at which mackinawite transforms. On cooling hexagonal FeS from high temperatures, magnetic ordering takes place before the $t\text{-Fe}_{1+x}\text{S}$ structure can form, with the result that the NiAs-type structure is retained. It is extremely unlikely, therefore, that in the pure FeS system, $t\text{-Fe}_{1+x}\text{S}$ will ever be prepared by cooling pure FeS.

It is possible that the addition of Co, Ni, or Cu in sufficient quantities may either increase the temperature of the $t\text{-Fe}_{1+x}\text{S}$ to FeS (NiAs) transition or lower the temperature at which magnetic ordering takes place in the FeS (NiAs) structure. Either effect might result in the tetragonal structure being favored energetically over the hexagonal structure, which may explain the (Cu, Co, Ni) FeS mackinawite obtained in dry synthesis experiments (Takeno et al., 1982).

ACKNOWLEDGMENTS

The authors wish to thank Barry Gale and Brian Smith for construction of the furnace used in these experiments. We thank M.E. Fleet for his constructive review, which helped to clarify interpretation of the data. This project was supported by NERC.

REFERENCES CITED

- Berner, R.A. (1962) Tetragonal FeS, a new iron sulfide. *Science*, 137, 669.
- (1964) Iron sulfides formed from aqueous solution at low temperatures and atmospheric pressure. *Journal of Geology*, 72, 293–306.
- Bertaut E.F., Bulet, P., and Chappert, J. (1965) Sur l'absence d'ordre magnetique dans la forme quadratique de FeS. *Solid State Communications*, 3, 335–338.
- Burke, J. (1965) The kinetics of phase transformations in metals, 226 p. Pergamon, Oxford, U.K.
- Cemič, L., and Kleppa, O.J. (1988) High temperature calorimetry of sulfide systems: III. Standard enthalpies of formation of phases in the systems Fe-Cu-S and Co-S. *Physics and Chemistry of Minerals*, 16, 172–179.
- Clark, A.H. (1966) Some comments on the composition and stability relations of mackinawite, *Neues Jahrbuch für Mineralogie Monatshefte*, 300–304.
- Covington, A.K., Bates, R.G., and Durst, R.A. (1985) Definition of pH scales, standard reference values, measurement of pH and related terminology. *Pure and Applied Chemistry*, 57, 531–542.
- Davison, W. (1991) The solubility of iron sulphides in synthetic and natural waters at ambient temperature. *Aquatic Sciences*, 53/4, 309–329.
- de Médecis, R. (1970a) Une nouvelle forme de sulfure de fer. *Revue de Chimie Minérale*, 7, 723–728.
- (1970b) Cubic FeS, a metastable iron sulfide. *Science*, 170, 1191–1192.
- Evans, H.T. (1970) Lunar troilite: Crystallography. *Science*, 167, 621–623.
- Evans, H.T., Berner, R.A., and Milton, C. (1962) Valleriite and mackinawite (abs.). Geological Society of America, Annual Meeting, p. 47A.
- Evans, H.T., Jr., Milton, C., Chao, E.C.T., Adler, I., Mead, C., Ingram, B., and Berner, R.A. (1964) Valleriite and the new iron sulfide, mackinawite. U.S. Geological Survey Professional Paper, 475-D, 64–69.
- Fagot, M., Levade, C., Conder, J.J., and Bras, J. (1981) Observation of lattice defects in orthorhombic iron disulphide (marcasite). *Physics and Chemistry of Minerals*, 7, 253–259.
- Fleet, M.E. (1970) Structural aspects of the marcasite-pyrite transformation. *Canadian Mineralogist*, 10, 225–231.
- (1975) Structural chemistry of marcasite and pyrite type phases. *Zeitschrift für Kristallographie*, 142, 332–346.
- Goodenough, J.B. (1978) Structural chemistry of iron sulfides. *Materials Research Bulletin*, 13, 1305–1314.
- Grønvold, F. (1968) Heat capacities and thermodynamic properties of the iron selenides Fe_{1.04}Se, Fe₂S₈ and Fe₃Se₄ from 298 to 1050°K. *Acta Chemica Scandinavica*, 22, 1219–1240.
- Grønvold, F., and Stølen, S. (1992) Thermodynamics of iron sulfides: II. Heat capacity and thermodynamic properties of FeS and of Fe_{0.875}S at temperatures from 298.15 K to 1000 K, of Fe_{0.98}S from 298.15 K to 800 K, and of Fe_{0.89}S from 298.15 K to about 650 K: Thermodynamics of formation. *Journal of Chemical Thermodynamics*, 24, 913–936.
- Hägg, G., and Sucksdorff, I. (1933) Die Kristallstruktur von Troilite und Magnetkies. *Zeitschrift für physikalische Chemie*, 22, 444–452.
- Hancock, J.D., and Sharp, J.H. (1972) Method of comparing solid-state kinetic data and its application to the decomposition of kaolinite, brucite and BaCO₃. *Journal of the American Ceramic Society*, 55, 74–77.
- Horwood, J.L., Townsend, M.G., and Webster, A.H. (1976) Magnetic susceptibility of single crystal Fe_{1-x}S. *Journal of Solid State Chemistry*, 17, 35–42.
- King, H.E., and Prewitt, C.T. (1982) High-pressure and high-temperature polymorphism of iron sulfide (FeS). *Acta Crystallographica*, B38, 1877–1887.
- Kjekshus, A., Nicholson, D.G., and Mukherjee, A.D. (1972) On the bonding in tetragonal FeS. *Acta Chemica Scandinavica*, 26, 1105–1110.
- Kouvo, O., Vuorelainen, Y., and Long, J.V.P. (1963) A tetragonal iron sulfide. *American Mineralogist*, 48, 511–524.
- Kruse, O. (1992) Phase transitions and kinetics in natural FeS measured by X-ray diffraction and Mössbauer spectroscopy at elevated temperatures. *American Mineralogist*, 77, 391–398.
- Lennie, A.R. (1994) Aspects of relations between metastable and stable phases in the iron-sulphur system. Ph.D. thesis, University of Manchester, Manchester, U.K.
- Lennie, A.R., and Vaughan, D.J. (1992) Kinetics of the marcasite-pyrite transformation: An infrared spectroscopic study. *American Mineralogist*, 77, 1166–1171.
- Murowchick, J.B., and Barnes, H.L. (1986) Formation of cubic FeS. *American Mineralogist*, 71, 1243–1246.
- Putnis, A. (1974) Electron-optical observations on the α -transformation in troilite. *Science*, 186, 439–440.
- (1992) Introduction to mineral sciences, 457 p. Cambridge University Press, Cambridge, U.K.
- Redfern, S.A.T. (1987) The kinetics of dehydroxylation of kaolinite. *Clay Minerals*, 22, 447–456.
- Robie, R.A., Hemingway, B.S., and Fisher, J.R. (1978) Thermodynamic properties of minerals and related substances at 298.15 K and 1 bar (10⁵ pascals) pressure and at higher temperatures. Geological Survey Bulletin, 1452, U.S. Government Printing Office, Washington, DC.
- Sarkar, S.C. (1971) Mackinawite from the sulfide ores of the Singbaom Copper belt, India. *American Mineralogist*, 56, 1312–1318.
- Schoonen, M.A.A., and Barnes, H.L. (1991a) Reactions forming pyrite and marcasite from solution: I. Nucleation of FeS₂ below 100°C. *Geochimica et Cosmochimica Acta*, 55, 1495–1504.
- (1991b) Reactions forming pyrite and marcasite from solution: II. Via FeS precursors below 100°C. *Geochimica et Cosmochimica Acta*, 55, 1505–1514.
- (1991c) Mechanisms of pyrite and marcasite formation from solution: III. Hydrothermal processes. *Geochimica et Cosmochimica Acta*, 55, 3491–3504.
- Schottky, W. (1922) Über die Drehung der Atomachsen in festen Körpern (Mit magnetischen, thermischen und chemischen Beziehungen). *Physikalische Zeitschrift*, 23, 448–455.
- Spiegel, M.R. (1991) Theory and problems of statistics (2nd edition), 504 p. McGraw-Hill, New York.
- Takeno, S. (1965a) A note on mackinawite (so-called valleriite) from the Kawayama mine, Japan. *Geological Reports, Hiroshima University*, 14, 59–76.
- (1965b) Thermal studies on mackinawite. *Journal of Science, Hiroshima University, Series C*, 4, 455–478.
- Takeno, S., and Clark, A.H. (1967) Observations on tetragonal (Fe, Ni, Co)_{1-x}S, mackinawite. *Journal of Science, Hiroshima University, Series C*, 5, 287–293.
- Takeno, S., Zōka, H., and Niihara, T. (1970) Metastable cubic iron sulfide—with special reference to mackinawite. *American Mineralogist*, 55, 1639–1649.
- Takeno, S., Moh, G.H., and Wang, N. (1982) Dry mackinawite syntheses. *Neues Jahrbuch für Mineralogie Abhandlungen*, 144(3), 297–301.
- Taylor, L.A., and Finger, L.W. (1970) Structural refinement and composition of mackinawite. *Carnegie Institute of Washington Geophysical Laboratory, Annual Report*, 69, 318–322.
- Taylor, P., and Shoesmith, D.W. (1978) The nature of the green alkaline iron sulfide solutions and the preparation of sodium iron (III) sulfide, NaFeS₂. *Canadian Journal of Chemistry*, 56(22), 2797–2802.
- Tsuji, T., Howe, A.T., and Greenwood, N.N. (1976) The Fe-Se system: I. Mossbauer spectra and electrical conductivity of Fe_{1.04}Se. *Journal of Solid State Chemistry*, 17, 157–163.
- Uda, M. (1968) The structure of tetragonal FeS. *Zeitschrift für Anorganische Chemie*, 361, 94–98.
- Vaughan, D.J., and Craig, J.R. (1978) Mineral chemistry of metal sulfides, 493 p. Cambridge University Press, Cambridge, U.K.
- Vaughan, D.J., and Ridout, M.S. (1971) Mössbauer studies of some sulfide minerals. *Journal of Inorganic and Nuclear Chemistry*, 33, 741–747.
- Ward, J.C. (1970) The structure and properties of some iron sulfides. *Reviews of Pure and Applied Chemistry*, 20, 175–206.

- Welz, D., and Rosenberg, M. (1987) Electronic band structure of tetrahedral iron sulphides. *Journal of Physics C: Solid State Physics*, 20, 3911-3924.
- Yund, R.A., and Hall, H.T. (1969) Hexagonal and monoclinic pyrrhotites. *Economic Geology*, 64, 420-423.
- Zōka, H., Taylor, L.A., and Takeno, S. (1972) Compositional variations in natural mackinawite and the results of heating experiments. *Journal of Science, Hiroshima University, Series C*, 7, 37-53.
- Zussman, J. (1977) X-ray diffraction. In J. Zussman, Ed., *Physical methods in determinative mineralogy* (2nd edition), 720 p. Academic, London.

MANUSCRIPT RECEIVED DECEMBER 7, 1994

MANUSCRIPT ACCEPTED MAY 15, 1995